7-log virus removal in a simple functionalized sand filter

Laxmicharan Samineni[a], Boya Xiong[b,1], Ratul Chowdhury[a,1], Andrew Pei[a], Louise Kuehster[d], Huiran Wang[a], Roman Dickey[a], Paula Espinoza Soto[a], Lynnicia Massenburg[c], Thanh H. Nguyen[e], Costas Maranas[a], Darrell Velegol[a], Manish Kumar[a, b, 2], Stephanie Velegol[a, 2]

[a]Department of Chemical Engineering, The Pennsylvania State University, University Park, Pennsylvania 16802, United States

[b]Department of Civil and Environmental Engineering, The Pennsylvania State University, University Park, Pennsylvania 16802, United States

[c]Department of Biochemistry and Molecular Biology, The Pennsylvania State University, University Park, Pennsylvania 16802, United States

[d]School of Chemical, Biological, and Materials Engineering, University of Oklahoma, Norman, Oklahoma 73019-1004, United States

[e]Department of Civil and Environmental Engineering, University of Illinois at Urbana-Champaign, Urbana, Illinois 61801, United States

[1]Both authors contributed equally to this manuscript

[2]Corresponding authors

Stephanie Velegol, Email: sbv1@psu.edu. Phone: +1 814-865-4907, Manish Kumar, Email: manish.kumar@psu.edu. Phone +1 814-865-7519.

Abstract: Viral contamination of drinking water due to fecal contamination is difficult to detect and treat effectively, leading to frequent outbreaks worldwide. The purpose of this paper is to report on the molecular mechanism for an unprecedented high virus removal from a practical sand filter. Sand filters functionalized using a water extract of *Moringa oleifera (MO)* seeds, *f*-sand filters, achieved ~7 $\log_{10}$ virus removal. These tests were conducted with MS2 bacteriophage, a recognized surrogate for pathogenic norovirus and rotavirus. We studied the molecular mechanism of this high removal since it can have important implications for sand filtration, the most common water treatment technology worldwide. Our data reveal that the virus removal activity of *f*-sand is due to the presence of a chitin binding protein – *Moringa oleifera* chitin binding protein (MoCBP) on *f*-sand. Standard column experiments were supported by proteomic analysis and molecular docking simulations. Our simulations show that MoCBP binds preferentially to MS2 capsid proteins demonstrating that specific molecular interactions are responsible for enhanced virus removal. In addition, we simplified the process of making *f*-sand and evinced how it could be regenerated using saline water. At present, no definitive solution exists for the challenge of treating fecally contaminated drinking and irrigation water for viruses without using technologies that demand high energy or chemical consumption. We propose functionalized sand (*f*-sand) filters as a highly effective, energy-efficient, and practical technology for virus removal applicable to both developing and developed countries.

Water-borne pathogen contamination and related health burden is a critical issue worldwide[1,2]. Acute diarrhea was responsible for 1.3 million deaths and 71.59 million DALYs (Disability Adjusted Life Years) globally in 2015[3]. Fecal contamination of water used for drinking, irrigation, and recreational purposes is responsible for waterborne transmission causing 88% of these diarrhea related deaths[4,5]. Although bacteria and protozoa can cause diarrhea, human enteric viruses (EVs) are the leading cause of acute diarrhea, with rotavirus alone attributing to 40% of the hospitalizations[6].

EVs pose higher health risk compared to bacteria and protozoa due to high concentrations shed by both symptomatic and asymptomatic patients[7-9], persistence in the environment[10-12], and an extremely low infectivity dose (the probability of infection is 31% with exposure to just one particle of rotavirus)[13-15]. Additionally, EVs are difficult to detect owing to their low background concentration in the environment, as well as resource, time, and labor intensive detection techniques[16,17]. While much attention has been paid to bacterial and protozoal infections from compromised water sources, viral infections remain hard to detect and combat[18].

Conventional filtration technologies used in most water treatment plants cannot filter viruses due to their small size. Previous studies on the two most commonly used filtration techniques, rapid sand filtration[19,20] and slow sand/ bio-sand filtration[21-23], indicated that they cannot achieve virus removals to meet drinking water standards (the US Environmental Protection Agency, EPA, requires 4 $\log_{10}$ removal of viruses[24]). Although membrane filtration techniques were shown to be effective against viruses[25-28], their widespread application is restricted due to high capital and operational costs[29-31]. In addition, membrane filtration needs near continuous monitoring of the integrity as any defects can brook the passage of viruses[32-35].

This lack of a reliable filtration technology leaves disinfection (chemical or UV) and boiling as the available options for protection against viral contamination. Of these, the practice of disinfection in centralized treatment and distribution systems has still resulted in cases of widespread infection[36-38]. Additionally, disinfection results in formation of disinfection byproducts, which may have cytotoxic and carcinogenic activity[39]. Boiling water is an energy intensive alternative which can be economically infeasible, especially in developing countries[40-42]. Therefore, there is a strong need for sustainable, energy-efficient water treatment techniques with virus removal capabilities.

To address this need, recent studies have focussed on improving the performance of membrane filtration technologies by functionalizing the surface of membranes using engineered nanoparticles (ENPs)[43-45] and cationic polymers or fabricating novel membranes using single/multi-walled carbon nanotubes[46,47] and nanocellulose materials[48-50]. Due to the use of ENPs and complicated casting methods, the environmental impact of production of these membranes can outweigh the benefits[51]. In contrast, there is a dearth of studies focused on enhancing the performance of the cornerstone technology in worldwide water treatment, sand filtration. We propose a simple filter built from natural materials (sand and plant seeds) that demonstrates enhanced removal of viruses from drinking water to address the challenges with current technologies.

Moringa oleifera (MO) is a deciduous tree which grows rapidly and widely in equatorial regions of the world, where the burden of access to safe drinking water is prominent[52]. As shown in **Fig. 1A,** *MO* is accessible in countries with the highest number of deaths of children under the age of five due to diarrhea caused by viral etiologies. The seeds of this tree contain cationic proteins with proven antimicrobial, antifungal, and coagulant activities[53-56], including the two proteins relevant to this study: *MO* coagulant protein (MO2.1)[53,55,57] and *MO* chitin binding protein (MoCBP)[56,58,59]. As a result, *MO* seeds have been traditionally used in indigenous water treatment[53,60]. Our previous work demonstrated that active proteins from *MO* could be adsorbed onto sand through electrostatic attraction[61]. This creates a net positively charged sand termed '*f*-sand' for particle and pathogen removal. Column filters made from *f*-sand achieved 3-4 $\log_{10}$ removal of model particles (1µm polystyrene) and > 8 $\log_{10}$ removal of *E. coli*[62] . Previous reports indicate that <1% of the annually produced seeds from one *MO* tree could suffice to fabricate a community scale *f*-sand filter[62]. The realization of full-scale implementation of this sustainable technology (*f*-sand filters) with virus removal capability that meets the drinking water standards could be an important step forward in addressing the viral contamination of drinking water.

In this work, we report high removal of virus (~7 $\log_{10}$ or 99.99999%) by *f*-sand filters coated with a simple *Moringa oleifera* aqueous seed extract and the corresponding molecular mechanism for removal. Bacteriophage MS2 was used as a surrogate for predicting the removal of EVs due to its structural similarities to EVs[63,64]. Our initial hypothesis was that *f*-sand filters might achieve enhanced virus removal compared to uncoated sand (bare sand) filters due to favorable electrostatic interactions. Indeed the *f*-sand filters remove ~7 $\log_{10}$ viruses. To further

understand the molecular mechanism of virus removal, a combination of mass spectrometry, gel electrophoresis, column experiments, and docking simulations were used. These results showed that the removal mechanism is based on specific interactions between the virus capsid proteins and MoCBP, a protein adsorbed on *f*-sand. We have thus identified an unprecedented, high virus removal in a simple protein-coated sand filter and elucidated the underlying molecular mechanism for this enhanced removal.

Further, in our pursuit towards facilitating the scale-up of *f*-sand columns, we report on a new and robust coating method (*in-situ* coating) for the *f*-sand columns along with a regeneration strategy using saline water. In addition, we tested the *in-situ* coating method with *MO* seeds from two different locations. Although developing countries are affected disproportionately, developed countries with state-of-art water treatment technologies are also susceptible to outbreaks of waterborne diseases. The *f*-sand filter represents a simple, scalable, low-energy system, for high virus removal from contaminated drinking or irrigation water, which may be applicable to multiple scenarios in developing and developed countries.

Materials and Methods

***Moringa oleifera* seeds:** Two batches of *Moringa oleifera* seeds from different origins were used in this work. Seed-A was received from Echo Global Farm, Florida. Seed-B was obtained from Nicaragua. Seed-A was used for all the experiments in the work except for the experiments performed to check the effect of seed origin. All seeds were stored at room temperature in a sealed bag and crushed before experiment for preparing *f*-sand columns to ensure that the technique was robust under practical conditions.

***f*- sand preparation (batch process)**: The batch process to prepare *f*-sand and the optimum amount of seed required to functionalize the sand surface (5.6 g/m^2) were adapted from our previous work[62]. Briefly, 3.1 g of unshelled whole *Moringa oleifera* seeds were crushed using a coffee grinder and mixed with 610 ml of deionized (DI) water for 5 minutes. The obtained water extract was filtered through 1.5 μm glass fiber filter (Whatman) and 0.22 μm PVDF filter (Millipore) to remove seed debris. 25 g unwashed glass beads of size ≤106 μm (model sand particles) were mixed with the seed extract for 5 minutes followed by settling for 5 minutes. The supernatant was discarded, and the glass beads were rinsed three times with DI water to remove

130 excess organic matter. The coated glass beads (*f*-sand) thus prepared were then used for packing
131 column filters to test removal of MS2. A schematic of the batch process to prepare *f*-sand is shown
132 in **Fig. 1B**.

133 **Column experiments:** We used readily available components to build the *f*-sand filters for
134 performing column experiments in this study. Glass chromatography columns (Bio-Rad) with 1.5
135 cm inner diameter and 10 cm length were used to perform column filtration experiments for
136 quantifying virus removal. A glass bead slurry coated with *Moringa oleifera* (*f*-sand) was poured
137 into the glass column and the column was rolled along its length, then set in an upright position
138 slowly to ensure that no trapping of air bubbles or layering occurred during packing. These
139 columns were packed overnight under gravity driven flow of sterilized DI water, followed by
140 equilibration with 1 mM NaCl (the background electrolyte used for diluting MS2 bacteriophage
141 stock) for 20 pore volumes. Once equilibration was completed, the inlet was switched to a $\approx 10^8$
142 PFU (Plaque Forming Unit)/ml MS2 solution in 1 mM NaCl. A constant flow rate was achieved
143 using a peristaltic pump with the influent charged to the top of the column. 1 ml effluent samples
144 were collected in sterilized micro-centrifuge tubes at 4, 6, and 8 pore volumes. Plaque assays of
145 influent and effluent samples were performed to analyze the concentration and subsequently the
146 removal efficiency[65]. Experimental log removal efficiency of viruses is calculated using **Eqn 1**,
147 where N, N_0 are effluent and influent sample concentrations.

148 $$\log \text{removal efficiency (LRE)} = -\log_{10}\left[\frac{N}{N_0}\right] \quad (1)$$

149 Whenever it is not specified, column experiments were performed using glass beads with size ≤
150 106 μm and a flow rate of 1.6 ml/min.

151 To understand the effect of flow rate on the LRE, flow rates of 1.6, 3.2, 4.8 ml/min were
152 tested using ≤ 106 μm glass beads. Next, collector size was varied by using glass beads of size ≤
153 106 μm, 212-300 μm, and 425-600 μm at a constant flow rate of 1.6 ml/min to understand the
154 effect of collector size on removal.

155 **MS2 propagation:** *Escherichia coli* bacteriophage MS2 (ATCC 15597-B1) was used as a
156 surrogate for enteric viruses to quantify virus removal in all our column experiments. MS2 was
157 obtained from the American Type Culture Collection and propagated using *Escherichia coli*

158 (ATCC 1597). First, an actively growing culture of *E. coli* was propagated in Tryptic Soy Broth;
159 inoculated with MS2 phage and incubated for 24 hours at 37 °C. After incubation, MS2 phage was
160 purified by centrifugation at 5000 rpm for 15 minutes at 4 °C, followed by filtration through 0.22
161 µm Durapore(R) PVDF membrane in Stericup®- HV filters. The stock solution of MS2 obtained
162 was diluted with equal parts of 50 % ethylene glycol: water mixture and separated into 1 ml
163 aliquots before storing at -80 °C. The frozen stock solution was thawed to room temperature before
164 dilution to the required concentration for column experiments.

165 **MS2 plaque assay:** To quantify the concentration of MS2 bacteriophage samples in terms
166 of plaque forming units per ml (PFU/ml) a double agar layer procedure (plaque assay) a standard
167 method to quantify virus infectious dose assay was used[65]. First, a single colony of *E. coli* was
168 inoculated into 10 ml Tryptic Soy Broth media and incubated for 6 hours at 37 °C to prepare the
169 *E. coli* solution for the plaque assay. 100 µl of this *E. coli* solution and 100 µl of the virus sample
170 were added to a liquid soft agar tube at 60 °C before pouring on to a base agar plate followed by
171 incubation at 37 °C for 12 hours. After the incubation, the concentration of MS2 bacteriophages
172 was determined by counting the number of transparent circles in the opaque bacterial lawn, which
173 represent the sites of MS2 infection. Except for the cases of very dilute effluent samples obtained
174 from column experiments, concentration was calculated as an average plaque count from plates
175 with 10-200 plaques.

176 **Gel electrophoresis:** To characterize the protein adsorbed on *f*-sand, Sodium Dodecyl
177 Sulfate Poly-Acryamide Gel Electrophoresis (SDS-PAGE)[66] evaluation was conducted by loading
178 12 µl of *f*-sand onto a 12 % hand-cast SDS PAGE gel. Coomassie staining was used to visualize
179 the protein bands. For protein identification, bands from the gel were incised, digested, and
180 analyzed at the Mass Spectrometry Core Facility at Penn State. Standard trypsin digestion
181 procedure was used for in-gel digestion.

182 **in-situ coating procedure:** One of the scale-up considerations discussed in this work is a
183 new and robust method for *in-situ* coating of the *f*-sand columns. Thermo Scientific™ Pierce™
184 Quantitative Fluorescent Peptide Assay (details of analysis are provided in *SI*) was used to quantify
185 the protein adsorbed on the sand particles. *MO* serum was fed to packed sand columns at a flow
186 rate of 1.6 ml/min using a peristaltic pump. We quantified the amount of protein adsorbed on sand
187 surfaces in three scenarios. Case 1: The batch mixing process previously used, Case 2: Single pass

188 *in-situ* coating using 60 ml *MO* seed extract (0.005 g seed/ml concentration) to reduce the water
189 and seed used by 10 times, and Case 3: Single pass *in-situ* coating using 15 mL of a four times
190 concentrated *MO* seed extract (0.02 g seed/ml) to further decrease the water consumption.

191 ***f-sand* filter regeneration:** Another consideration for scale-up discussed in this work is
192 the capability of regenerating the *f*-sand columns. To show regeneration capability, *f*-sand columns
193 using ≤106 μm glass beads were first coated using the *in-situ* coating discussed above and then
194 washed with 100 ml of 600 mM NaCl to desorb the protein before re-coating them for three cycles.
195 The MS2 removal efficiency of the washed and re-coated columns was quantified for each cycle
196 to study at a constant flow rate of 1.6 ml/min.

197 **N-Acetyl D-Glucosamine (GlcNAc) blocking experiments**: To test the hypothesis that
198 specific interactions between the chitin binding region of MoCBP and MS2 are responsible for the
199 observed MS2 removal, we performed experiments with *f*-sand columns made from Seed-A by
200 implementing a wash step with GlcNAc. 100 ml solution of 1M GlcNAc in 10 mM phosphate
201 buffer (pH = 7.0) was used to target the possible saturation of the chitin binding regions in MoCBP,
202 before filtering MS2. To compare the performance of columns washed with GlcNAc with the *f*-
203 sand filters, ≤106 μm glass beads were used as collectors to pack the columns and the MS2 removal
204 efficiency was quantified at a constant flow rate of 1.6 ml/min.

205 **Results and Discussion**

206 ***f*-sand filters achieved ~ 7 $\log_{10}$ removal of virus particles.** Column experiments were performed
207 using crude water extract from *MO* seeds to functionalize ≤106 μm glass beads (model sand
208 particles) using the batch process of coating to measure MS2 removal in *f*-sand filters. Column
209 filters packed with uncoated glass beads (bare sand filters) were used as a negative control to
210 represent the performance of a model conventional sand filter. The *f*-sand filters achieved a $\log_{10}$
211 removal efficiency (LRE) of 7.0 ± 0.5 for MS2 particles compared to 0.2 ± 0.1 demonstrated by
212 bare sand filters at a flow rate of 1.6 ml/min (**Fig. 2A)**. This enhanced removal achieved by the *f*-
213 sand filter clearly indicates favorable interactions between *f*-sand and MS2 particles. This removal
214 is three orders of magnitude higher than the US EPA mandated virus removal (4 $\log_{10}$); which is
215 currently achieved using multiple steps of coagulation, filtration, and chemical or UV disinfection
216 in water treatment plants. In particular, *f*-sand filter performance exceeds that of conventional sand

filters with a precoagulation step (1-2 $\log_{10}$)[19,20], and slow sand filters (1-4 $\log_{10}$)[21-23]. The performance of these filters is on par with the removals achieved using membrane filtration techniques such as ultrafiltration[67,68], reverse osmosis[28], as well as novel filtration techniques based on functionalization of low-pressure membrane surfaces with antimicrobial engineered nanoparticles or cationic polymers[43-45], size exclusion membranes made of carbon nanotubes[46,47], and nano-cellulose fibers[48-50]. However, unlike these methods the use of *f*-sand filters does not involve the use of chemicals, nanoparticles, or complicated membrane casting methods.

Column experiments were performed by varying flow rate and collector (glass bead) diameter to gain insights into the effect of flow rate and collector size on the removal efficiency of the *f*-sand filters. As shown in **Fig. S1**, an increase in flow rate or collector diameter decreases the removal efficiency. These experimental results indicate that flow rate within the studied range can be used as a tunable parameter to achieve the required virus removal performance with these filters.

MoCBP and MO2.1 are the two proteins adsorbed on *f*-sand. To identify the molecular mechanism of virus removal in *f*-sand filters we started with characterizing the proteins adsorbed onto the sand surface. To accomplish this, we performed SDS-PAGE analyses on the proteins desorbed from *f*-sand. As shown in **Fig. 2B**, the *f*-sand shows three main bands at ~15kDa, ~18kDa and ~36kDa. We further made a single incision (to account for interfering bands) of the lane from 15kDa to 40kDa in a gel similar to the one shown in **Fig. 2B** and performed mass spectrometry analysis at the Penn State Proteomics and Mass Spectrometry Core Facility, University Park, PA. Mass spectrometry analysis indicated the presence of two proteins MO2.1 and MoCBP on *f*-sand. MO2.1 is a 6.5kDa protein and exists as a homodimer of 13kDa[55] and sometimes also as a tetramer[57]. MoCBP is a ~14kDa protein with antifungal activity and chitin binding activity[56]. Previous work showed that MoCBP migrates anomalously at ~18kDa in non-reducing gel electrophoresis because of its carbohydrate binding activity[56]. As shown in **Fig. 2C**, there is a high degree of sequence similarity between the reported sequences of MO2.1 and MoCBP. Specifically, 54 out of 60 residues present in MO2.1 are conserved completely with the MoCBP sequence. Nonetheless, MO2.1 and MoCBP are shown as distinct proteins in the literature as MoCBP is a heterodimer of a ~8kDa long chain and a ~4kDa short chain, whereas MO2.1 was reported to exist as a homodimer of a 6.5kDa monomer[59].

Once we identified the presence of two distinct proteins on *f*-sand, we sought to identify which of these two proteins (MoCBP or MO2.1) was responsible for MS2 removal and to discern the specific mechanism of removal. To this end, we performed *in silico* binding experiments, and blocking experiments which are discussed in the next two sections.

***In silico* binding experiments showed that MoCBP interacts favorably with MS2 capsid protein.** We performed *in silico* binding experiments between MS2 capsid protein and the two proteins (MoCBP and MO2.1) to determine the molecular mechanism of virus removal. In **Fig. 3**, we show the docking regions involved in the interaction of MS2 with MoCBP and MO2.1 along with the *in silico* interaction energies (binding free energy). Details of the MoCBP-MS2 residue level interactions are shown in Supplementary **Fig. S4** and tabulated in Supplementary **Table S1**. Investigation of these detailed molecular interactions reveal that MoCBP-MS2 binding is predominantly electrostatic (41 interactions), as well as some that are strongly hydrogen-bonded (6 interactions) and local hydrophobically packed regions at the interface (5 interactions) (details in Supplementary **Fig. S4**). These results indicate that MoCBP interacts favorably with the MS2 capsid protein with an interaction energy of -220.4 kcal/mol. In contrast, the interaction between MO2.1 and MS2 is thermodynamically unfavorable with an interaction energy of 11.1 kcal/mol. MO2.1 serves as an *in silico* negative control, as even though there is a high sequence similarity with MoCBP, the absence of the flexible loop prevents it from offering a suitable surface to bind MS2. Consequently, we hypothesize that MoCBP present on *f*-sand was responsible for MS2 removal. There are four precursor MoCBP sequences[59] and one crystal structure for mature-MoCBP[69] available in literature. Our docking simulations indicated favorable interactions between MS2 and all the reported MoCBP variants with an average interaction energy of -290.7 kcal/mol (**Fig. S2**) involving similar binding regions (**Fig. S3)**.

GlcNAc blocking experiments further ascertain that specific interactions between MS2 and MoCBP is the mechanism of MS2 removal. MoCBP, is a thermostable cationic protein with demonstrated *in vitro* antifungal activity against various phytogenic fungi, even after heating at 100 °C for 1 hour[56]. The mode of this activity was shown to be alterations in the cell surface of fungus causing morphological changes and eventually cell death induced by oxidative stress[58]. Moreover, MoCBP can be purified from water extract of *MO* seeds using chitin column chromatography[56]. Therefore, due to the interaction of MoCBP with the fungal cell wall, in which

chitin is a primary component, and its affinity in chitin column chromatography, MoCBP was hypothesized to contain a chitin binding site. Chitin is a long chain polymer of GlcNAc, which is a glucose derivative.

We hypothesized that the chitin binding site of MoCBP is responsible for the favorable interactions with MS2 capsid protein. To test this hypothesis, we first performed *in-silico* molecular docking simulations[70,71] to understand the interactions of MoCBP with MS2 virus and GlcNAc. As the interaction energies and binding regions for different MoCBP variants and MS2 were very similar (**Fig. S2, Fig. S3**), we used one variant of MoCBP (variant 2) for the docking simulations with GlcNAc. The results from the docking simulations show that MoCBP interacts favorably, through electrostatic interactions with specific residues, with both MS2 and GlcNAc through two binding regions (BP1, BP2) as shown in **Fig. 4A** and **4B**. The binding residues in MoCBP that favorably interact with MS2 and GlcNAc overlap as shown in **Fig. 4C**. According to previous literature, amino acid residues 70 through 90 of MoCBP were hypothesized to constitute a linker peptide, which is proteolytically cleaved during the processing of precursor protein[59]. Note that the first chitin binding pocket (BP1) from docking simulations overlaps partially with the linker peptide.

Docking simulation results also show that the interaction energy of MoCBP with GlcNAc (-890.2 kcal/mol) is more negative compared to MS2 (-220.4 kcal/mol), suggesting a potential competition between MS2 and GlcNAc (**Fig. 4D**). Thus, we hypothesized that blocking the chitin-binding site of MoCBP with GlcNAc should inhibit further MS2 binding, reducing the overall removal of MS2. To test this hypothesis, we performed experiments with *f*-sand columns by implementing a wash step with GlcNAc. *f*-sand filters without washing were used as a positive control. This way of verfying that MoCBP is responsible for MS2 removal by GlcNAc washing was specifically employed to understand the mechanism under conditions relevant to practical applications of *f*-sand filters and account for any MO2.1 interference effects. As expected, the GlcNAc washed *f*- sand filters lose the capability of removing MS2 (**Fig. 4E**). This confirms our hypothesis that the virus removal activity is due to the chitin binding region present in *MO* seed aqueous extract.

In this work, we show that *f*-sand filters can be used to achieve effective removal of virus

particles from water and elucidated the underlying molecular mechanism. These findings, in conjunction with our previous work showing *E. coli* removal with *f*-sand filters, establish *f*-sand filters as a potential low-cost, sustainable pathogen removal technology. In the next section, we report scale-up considerations such as reduction in seed and water, variability in seed origin, and a rapid regeneration process for *f*-sand filters.

Scale-up considerations for *f*-sand filters:

The batch process for preparing lab-scale *f*-sand columns requires 610 ml of *MO* water extract (0.005 g seed/ml) consuming 3.05 g of *MO* seed to coat 25 g of sand. In addition, this technique requires constant mixing for protein extraction of crushed seed and simultaneous coating of sand particles. Our goal was to simplify this process and use lower amounts of seeds and water. *In-situ* coating of the sand filter by flowing MO serum through columns is a more efficient way to coat sand, because the mixing obtained will be higher without requiring external equipment. We hypothesized that *in-situ* coating of prepared sand columns will increase the ease and robustness of preparing *f*-sand columns at the lab and field scales. To test this hypothesis, we quantified the amount of protein adsorbed on sand surfaces in three scenarios. Case 1: The batch mixing process previously used, Case 2: Single pass *in-situ* coating using 10 times less seed and water, and Case 3: Single pass *in-situ* coating using 40 times less water and 10 times less seed. As shown in **Fig. 5A**, the amount of protein adsorbed on *f*-sand using the *in-situ* coating procedure with 15 ml of the concentrated *MO* serum was approximately 5 times higher compared to the batch process. This new and improved coating procedure decreases the amount of seed and water usage and eliminates the need for physical mixing.

After the *in-situ* coating procedure was established, the second scale-up consideration was the variability *MO* seed origin. Column experiments were conducted with ≤106 μm glass beads at a flowrate of 1.6 ml/min using Seed-A and Seed-B (origins are mentioned in materials section). As shown in **Fig. 5B**, the columns made using both Seed-A and Seed-B achieve similar removals of MS2 particles. This indicates that *f*-sand filter technique is robust and has a potential to be applied widely across world with locally accessible *MO* seeds.

The third scale-up consideration is the regeneration and reuse of *f*-sand columns. Previous work established that 600 mM NaCl can be used to desorb MO proteins from sand surface[72]. This

combined with the proposed *in-situ* coating can provide an avenue to reuse columns. Desorbing exhausted proteins from sand and re-coating using *in-situ* coating eliminates the need for making new columns after eventual column breakthrough. To show regeneration capability, *f*-sand columns were first coated using *in-situ* coating and then washed with 100 ml of 600 mM NaCl before re-coating them. This process was repeated three times and the MS2 removal efficiency of the washed and re-coated columns was quantified for each cycle. The results (**Fig. S5)** show that we can successfully regenerate the *f*-sand columns using this method to achieve EPA required virus removal (4-log) for all three cycles.

In summary, the primary pupose of this paper was to elucidate the molecular mechanism of virus removal using *f*-sand filter technology. This could lead to a practical way to enhance the pathogen removal of conventional sand filtration. Future work is needed for full practical implementation of this technology. This future work needs to include an investigation of the impact of naturally occuring organic matter on the generation and re-generation of *f*-sand as well as the performance and lifetime of the filters. In addition, we will study the use of binary mixtures of sand sizes to mimic the hydraulic conductivity and residence time of this filter and further investigate the quality of the seed. Finally, long term experiments will allow predictions on the lifetime of the filter. Previous work using 1 μm sPSL particles showed that breakthough occurs when 5% of the surface is covered with particles.[62] If this holds for viruses, the breakthough of viruses would take on the order of years because viruses are much smaller than these particles. However, the presence of other components in the water such as organic matter, multivalent salts and other microorganisms will impact the lifetime of these filters. In addition to applications in sand filtration, this technique can be easily translated to other filter media to sustainably enhance the performance of various other filtration techniques (membrane filtration, diatomaceous earth) due to the uncomplicated and cost-effective functionalization process.

ACKNOWLEDGEMENTS. The authors would like to thank Andrew Erdman for providing *Moringa* seeds. The authors acknowledge Dr. Tatiana Laremore for the help with sample preparation for and data interpretation of mass spectrometric analysis. The authors would like to thank Prof. B.Tracy Nixon for helpful discussions about affinity column chromatography. The authors would like to thank Dr. Tammy Wood for providing the florescent *E. coli* strain. This work

was supported in part by funding from National Science Foundation project (CBET-1705278). Additional funding support was provided by Department of Chemical Engineering at Pennsylvania State, a National Science Foundation REU program (EEC-1659497) and Pennsylvania State University Global Programs.

Supporting information: Methods and materials for fluorometric peptide assay to quantify the amount of protein adsorbed on *f*-sand are available in the supporting information. The protein data bank (.pdb) files for the 3-dimensional structures of *Moringa oleifera* chitin binding protein (MoCBP) variants, homology modeled *Moringa oleifera* coagulant protein (MO2.1), MS2 capsid protein (PDB: 1AQ3) and GlcNAc used in this study are also available in the supporting information.

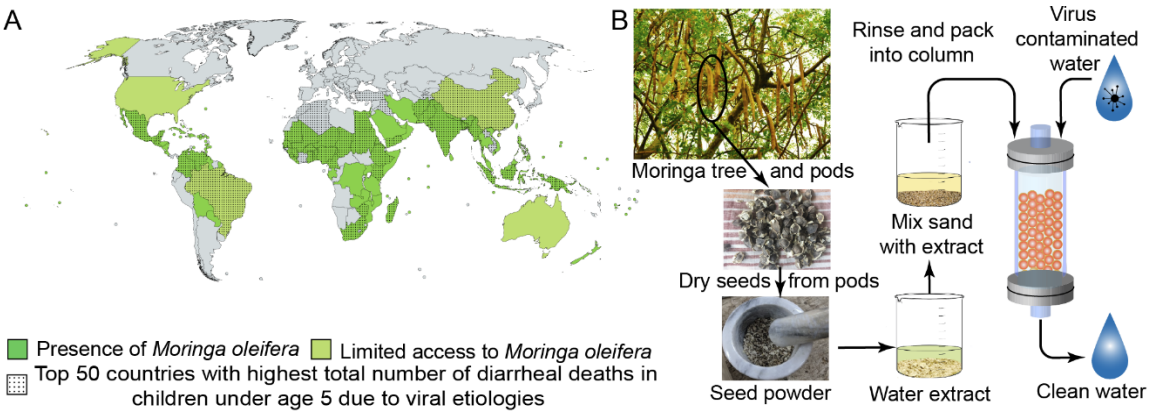

Figure 1. ***Moringa oleifera (MO)*** **is readily accessible in countries with the highest number of total deaths in children under age 5 due to diarrhea caused by viral etiologies.** ***MO*** **seed extract can be developed into a sustainable virus removal water filter. A)** The geographical distribution of *MO* was plotted based on the data from Centre of Agriculture and Business International datasheet[73]. Note that in some cases, *MO* presence is reported in only specific parts of the country and is represented as countries with limited accessibility such as the United States. This figure also shows the total number of deaths in children under age-5 due to diarrhea caused by viral etiologies (norovirus, rotavirus, and adenovirus (serotypes 40, 41)) as reported based on Global Burden of Disease, 2015[3] and was used to rank 195 countries based on the number of deaths. An overlay of the *MO* presence and top 50 countries with the highest number of deaths shows that *MO* is readily accessible in most of these countries. The world map was created using mapchart.net. **B)** A simple functionalization procedure using *MO* seed water extract was used to improve the pathogen removal efficiency of sand filters. A typical procedure involving water extraction of active proteins from crushed seed powder followed by filtration to remove seed debris. Then the water extract is mixed with sand particles to preferentially adsorb the active protein onto the sand surface. This *f*-sand was packed into glass columns to prepare *f*-sand filters. Images of *MO* tree and pods by Prof. Chen Hualin[74]. Reprinted/Adapted from https://commons.wikimedia.org/wiki/File:The_tree_and_seedpods_of_Moringa_oleifera.JPG. Accessed on 10/07/2019. under the Creative Commons Attribution-Share Alike 4.0 International license. Copyright 2015, own work.

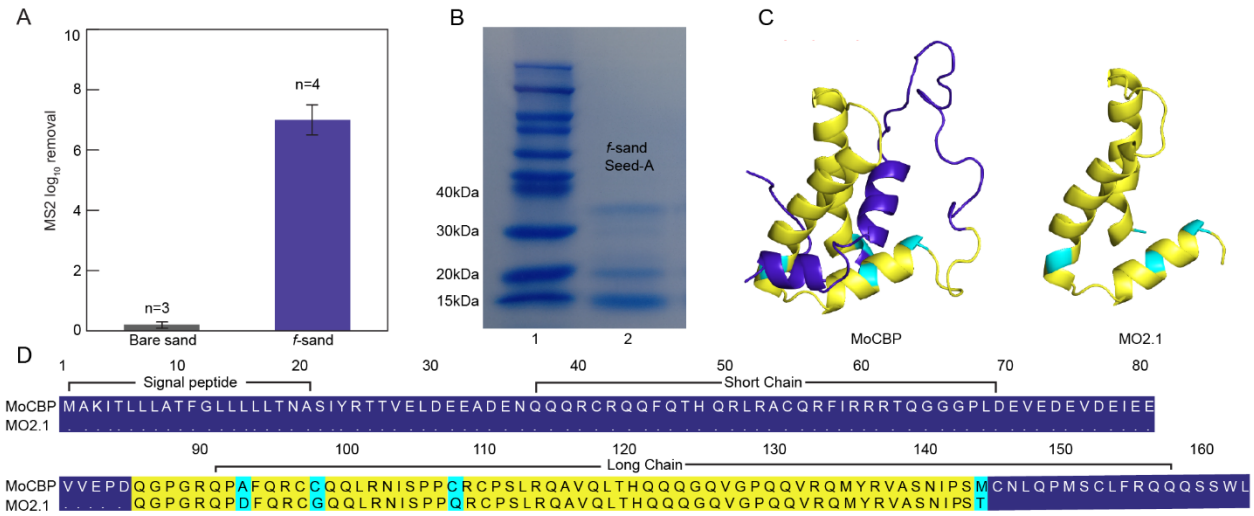

Figure 2. *MO* aqueous seed extract adsorbed onto sand (*f*-sand) shows significant virus removal compared to uncoated sand. SDS-PAGE gel and mass spectrometry revealed the presence of two proteins, MoCBP and MO2.1 on the sand, that share significant sequence similarity. A) Experimental $\log_{10}$ removal of 10^8 PFU/mL MS2 bacteriophage influent using *f*-sand filters made from Seed-A compared to that of uncoated sand filters (collector size of 106 µm and flow rate of 1.6 mL/min) show that *f*-sand filters made with Seed-A achieve orders of magnitude higher (7.1±0.4 $\log_{10}$) removal of MS2 particles compared to bare sand filters (0.2±0.05 $\log_{10}$), indicating favorable interactions between the adsorbed proteins and MS2 capsid. **B)** SDS-page gel electrophoresis of *f*-sand made from both Seed-A and Seed-B show three major bands (Lanes: 1- protein ladder, 2- *f*-sand made from Seed-A, 3- *f*-sand made from Seed-B). Mass spectrometry analysis of the bands from the gel showed the presence of two proteins: MoCBP and MO2.1 on *f*-sand. **C)** Homology models for MoCBP and MO2.1 used in this study and sequence data show their high structural and sequence similarity. A local sequence alignment shows the overall conserved motif in yellow interspersed by four non-conserved residue positions highlighted in cyan. **D)** The amino acid sequence of MoCBP precursor (AHG99683.1) is aligned with a reported sequence of MO2.1(P24303.1) using ClustalW. 56 out of 60 amino acid positions present in MO2.1 are conserved in MoCBP (color scheme is the same as homology models).

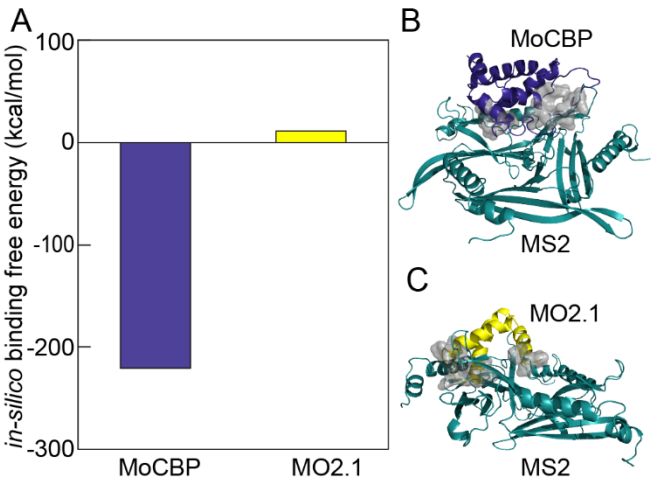

Figure 3. *In silico* binding experiments suggest that MoCBP is the protein responsible for MS2 removal. A) Comparison of *in silico* binding free energies of MoCBP and MO2.1 with MS2 obtained from docking simulations. MoCBP shows a favorable interaction with MS2 capsid protein (-220.4 kcal/mol) whereas the molecular interaction between MO2.1 and MS2 is thermodynamically unfavorable (11.1 kcal/mol). These results suggest that out of the two proteins present on *f*-sand, MoCBP binds preferentially to MS2 and suggests that MoCBP adsorbed on sand is responsible for its virus removal activity. The regions of MoCBP **(B)** and MO2.1 **(C)** interacting with MS2 obtained from the docking simulations used to calculate the binding free energy is represented as a gray surface while the MS2 capsid protein, MO2.1 and MoCBP are shown in teal, yellow and blue respectively.

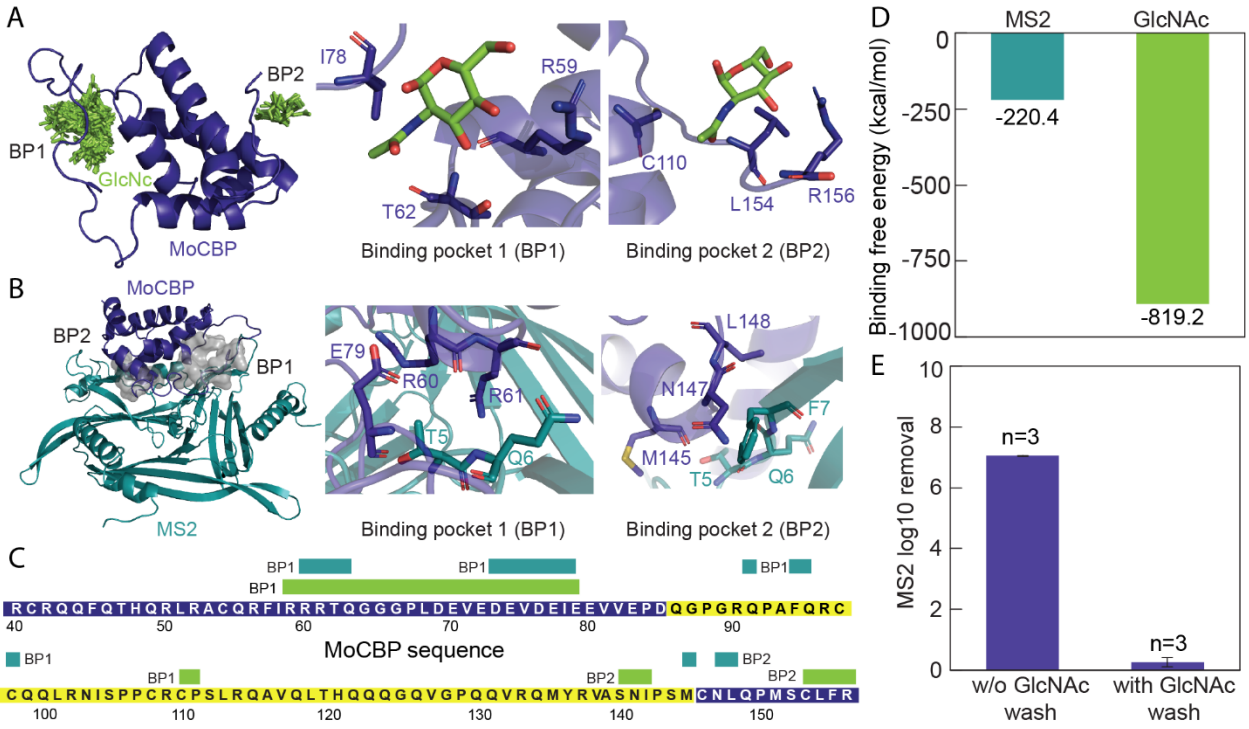

Figure 4. Favorable interactions between MoCBP and the MS2 capsid protein through its proposed chitin-binding region, is the mechanism of MS2 removal in *f*-sand filters. A) Molecular docking simulation results for interaction between MoCBP and GlcNAc (chitin monomer) show the regions of MoCBP with favorable electrostatic contacts. Some of the residues are within hydrogen-bonding distances (<3.5 Å) while the rest can contribute to weak electrostatic interactions (< 6.5 Å). See details in supplementary information **Fig. S6** and **Table. S1**. **B)** Molecular docking simulation results for interaction between MoCBP and MS2 show the regions of MoCBP showing favorable electrostatic interactions. **C)** The binding sites of MoCBP with MS2 and GlcNAc are shown in the sequence of MoCBP indicating the overlap of the binding regions. This indicates the possible competition for adsorption between them. **D)** *In silico* binding free energies for MS2 and GlcNAc with MoCBP from energy-minimized structures reveal GlcNAc exhibits much stronger interaction with MoCBP compared to MS2. This suggests a possible competition for binding between MS2 and GlcNAc which is used to design experiments. **E)** Experimental $\log_{10}$ removal of 10^8 PFU/mL MS2 bacteriophage using *f*-sand filters made from Seed-A compared to the *f*-sand filters from Seed-A washed with GlcNAc. GlcNAc washing inhibits the virus removal activity of *f*-sand filters made from Seed-A. These results show that the chitin binding region of MoCBP is the active site responsible for virus removal and that specific interactions between MS2 and MoCBP is the mechanism of removal. All the error bars shown in the figure represent the standard error calculated from three independent measurements (n=3).

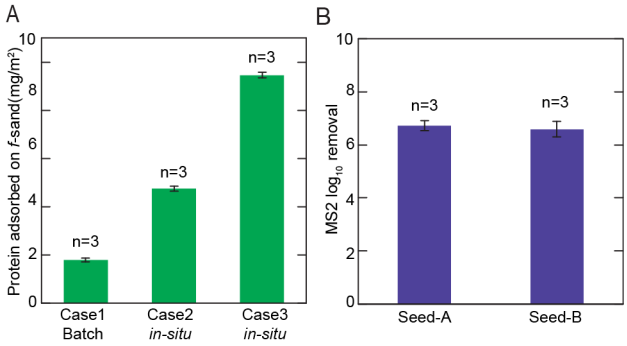

Figure 5. The *in-situ* coating method is an efficient and robust way to prepare *f*-sand columns. *f*-sand columns made using this coating method and *MO* seeds originating from different locations show similar MS2 removal A) The amount of protein adsorbed on sand surface for three coating situations 1) Case1: Batch process 2) Case2: *In-situ* coating by flowing 60 ml of *MO* serum of same concentration as batch process (0.005 g seed/ml) through each column 3) Case3: *In-situ* coating by flowing 15 ml of concentrated *MO* serum (0.02 g seed/ml) through each column. Protein quantification show that *in-situ* coating with concentrated *MO* serum is an efficient and robust coating method and the amount of protein adsorbed can be increased ~5 times following this process **B)** Experimental $\log_{10}$ removal of 10^8 PFU/mL MS2 bacteriophage influent using *f*-sand filters made from Seed-A compared to that made from Seed-B using the in-situ coating method (collector size of 106 μm and flow rate of 1.6 mL/min) show that Seed-A (6.72±0.19 $\log_{10}$) and Seed-B (6.59±0.3 $\log_{10}$) achieve similar removal of MS2 particles.

References:

(1) Gill, S.; Hayes, J.; Coates, S. Diarrhoea dialogues: From policies to progress. A call for urgent action to prevent the biggest killer of children in sub-Saharan Africa. **2012**.

(2) Bartsch, S. M.; Lopman, B. A.; Ozawa, S.; Hall, A. J.; Lee, B. Y. Global economic burden of norovirus gastroenteritis. *PloS one* **2016**, *11*, e0151219.

(3) Troeger, C.; Forouzanfar, M.; Rao, P. C.; Khalil, I.; Brown, A.; Reiner Jr, R. C.; Fullman, N.; Thompson, R. L.; Abajobir, A.; Ahmed, M. Estimates of global, regional, and national morbidity, mortality, and aetiologies of diarrhoeal diseases: a systematic analysis for the Global Burden of Disease Study 2015. *The Lancet Infectious Diseases* **2017**, *17*, 909-948.

(4) Black, R. E.; Morris, S. S.; Bryce, J. Where and why are 10 million children dying every year? *The lancet* **2003**, *361*, 2226-2234.

(5) UNICEF.: *Progress for children: a report card on water and sanitation*; UNICEF, 2006.

(6) Organization, W. H. Global networks for surveillance of rotavirus gastroenteritis, 2001-2008. *Weekly Epidemiological Record= Relevé épidémiologique hebdomadaire* **2008**, *83*, 421-425.

(7) Bozkurt, D.; Selimoglu, M. A.; Otlu, B.; Sandikkaya, A. Eight different viral agents in childhood acute gastroenteritis. *The Turkish journal of pediatrics* **2015**, *57*, 68.

(8) Schultz-Cherry, S.: *Astrovirus research: essential ideas, everyday impacts, future directions*; Springer Science & Business Media, 2012.

(9) Atmar, R. L.; Opekun, A. R.; Gilger, M. A.; Estes, M. K.; Crawford, S. E.; Neill, F. H.; Graham, D. Y. Norwalk virus shedding after experimental human infection. *Emerging infectious diseases* **2008**, *14*, 1553.

(10) Fong, T.-T.; Lipp, E. K. Enteric viruses of humans and animals in aquatic environments: health risks, detection, and potential water quality assessment tools. *Microbiol. Mol. Biol. Rev.* **2005**, *69*, 357-371.

(11) Kutz, S.; Gerba, C. P. Comparison of virus survival in freshwater sources. *Water Science and Technology* **1988**, *20*, 467-471.

(12) Reynolds, K. A.; Mena, K. D.; Gerba, C. P.: Risk of waterborne illness via drinking water in the United States. In *Reviews of environmental contamination and toxicology*; Springer, 2008; pp 117-158.

(13) Hall, A. J.: Noroviruses: the perfect human pathogens? ; Oxford University Press, 2012.

(14) Couch, R. B.; Cate, T. R.; Douglas Jr, R. G.; Gerone, P. J.; Knight, V. Effect of route of inoculation on experimental respiratory viral disease in volunteers and evidence for airborne transmission. *Bacteriological reviews* **1966**, *30*, 517.

(15) Ward, R. L.; Bernstein, D. I.; Young, E. C.; Sherwood, J. R.; Knowlton, D. R.; Schiff, G. M. Human rotavirus studies in volunteers: determination of infectious dose and serological response to infection. *Journal of Infectious Diseases* **1986**, *154*, 871-880.

(16) Gerba, C. P.; Betancourt, W. Q.; Kitajima, M.; Rock, C. M. Reducing uncertainty in estimating virus reduction by advanced water treatment processes. *Water research* **2018**, *133*, 282-288.

(17) Haramoto, E.; Kitajima, M.; Hata, A.; Torrey, J. R.; Masago, Y.; Sano, D.; Katayama, H. A review on recent progress in the detection methods and prevalence of human enteric viruses in water. *Water research* **2018**, *135*, 168-186.
(18) Gall, A. M.; Mariñas, B. J.; Lu, Y.; Shisler, J. L. Waterborne viruses: a barrier to safe drinking water. *PLoS pathogens* **2015**, *11*, e1004867.
(19) Shirasaki, N.; Matsushita, T.; Matsui, Y.; Yamashita, R. Evaluation of the suitability of a plant virus, pepper mild mottle virus, as a surrogate of human enteric viruses for assessment of the efficacy of coagulation–rapid sand filtration to remove those viruses. *Water research* **2018**, *129*, 460-469.
(20) Asami, T.; Katayama, H.; Torrey, J. R.; Visvanathan, C.; Furumai, H. Evaluation of virus removal efficiency of coagulation-sedimentation and rapid sand filtration processes in a drinking water treatment plant in Bangkok, Thailand. *Water research* **2016**, *101*, 84-94.
(21) Yahya, M.; Cluff, C.; Gerba, C. Virus removal by slow sand filtration and nanofiltration. *Water Science and Technology* **1993**, *27*, 445-448.
(22) Poynter, S.; Slade, J. In *Tilte*1978; Elsevier.
(23) Guchi, E. Review on slow sand filtration in removing microbial contamination and particles from drinking water. *American Journal of Food and Nutrition* **2015**, *3*, 47-55.
(24) Environmental, P. A. E. National primary drinking water regulations: Long Term 1 Enhanced Surface Water Treatment Rule. Final rule. *Federal register* **2002**, *67*, 1811.
(25) Fiksdal, L.; Leiknes, T. The effect of coagulation with MF/UF membrane filtration for the removal of virus in drinking water. *Journal of Membrane Science* **2006**, *279*, 364-371.
(26) Madaeni, S.; Fane, A.; Grohmann, G. Virus removal from water and wastewater using membranes. *Journal of Membrane Science* **1995**, *102*, 65-75.
(27) Urase, T.; Yamamoto, K.; Ohgaki, S. Effect of pore structure of membranes and module configuration on virus retention. *Journal of Membrane Science* **1996**, *115*, 21-29.
(28) Adham, S. S.; Trussell, R. S.; Gagliardo, P. F.; Trussell, R. R. Rejection of MS-2 virus by RO membranes. *Journal-American Water Works Association* **1998**, *90*, 130-135.
(29) Alzahrani, S.; Mohammad, A. W. Challenges and trends in membrane technology implementation for produced water treatment: A review. *Journal of Water Process Engineering* **2014**, *4*, 107-133.
(30) Zularisam, A.; Ismail, A.; Sakinah, M. Application and challenges of membrane in surface water treatment. *J. Appl. Sci* **2010**, *10*, 380-390.
(31) Adham, S. S.; Jacangelo, J. G.; Laîné, J. M. Characteristics and costs of MF and UF plants. *Journal-American Water Works Association* **1996**, *88*, 22-31.
(32) Kumar, M.; Adham, S.; DeCarolis, J. Reverse osmosis integrity monitoring. *Desalination* **2007**, *214*, 138-149.
(33) Adham, S.; Gagliardo, P.; Smith, D.; Ross, D.; Gramith, K.; Trussell, R. Monitoring the integrity of reverse osmosis membranes. *Desalination* **1998**, *119*, 143-150.
(34) Pearce, G. Water and wastewater filtration: Membrane module format. *Filtration & separation* **2007**, *44*, 31-33.
(35) Pype, M.-L.; Lawrence, M. G.; Keller, J.; Gernjak, W. Reverse osmosis integrity monitoring in water reuse: The challenge to verify virus removal–A review. *Water research* **2016**, *98*, 384-395.

(36) Payment, P. Poor efficacy of residual chlorine disinfectant in drinking water to inactivate waterborne pathogens in distribution systems. *Canadian journal of microbiology* **1999**, *45*, 709-715.
(37) Lee, E. J.; Schwab, K. J. Deficiencies in drinking water distribution systems in developing countries. *Journal of water and health* **2005**, *3*, 109-127.
(38) Ercumen, A.; Gruber, J. S.; Colford Jr, J. M. Water distribution system deficiencies and gastrointestinal illness: a systematic review and meta-analysis. *Environmental Health Perspectives* **2014**, *122*, 651-660.
(39) Richardson, S. D.; Plewa, M. J.; Wagner, E. D.; Schoeny, R.; DeMarini, D. M. Occurrence, genotoxicity, and carcinogenicity of regulated and emerging disinfection by-products in drinking water: a review and roadmap for research. *Mutation Research/Reviews in Mutation Research* **2007**, *636*, 178-242.
(40) Gilman, R. H.; Skillicorn, P. Boiling of drinking-water: can a fuel-scarce community afford it? *Bulletin of the World Health Organization* **1985**, *63*, 157.
(41) Shrestha, K. B.; Thapa, B. R.; Aihara, Y.; Shrestha, S.; Bhattarai, A. P.; Bista, N.; Kazama, F.; Shindo, J. Hidden Cost of Drinking Water Treatment and Its Relation with Socioeconomic Status in Nepalese Urban Context. *Water* **2018**, *10*, 607.
(42) Clasen, T.; McLaughlin, C.; Nayaar, N.; Boisson, S.; Gupta, R.; Desai, D.; Shah, N. Microbiological effectiveness and cost of disinfecting water by boiling in semi-urban India. *The American journal of tropical medicine and hygiene* **2008**, *79*, 407-413.
(43) Zodrow, K.; Brunet, L.; Mahendra, S.; Li, D.; Zhang, A.; Li, Q.; Alvarez, P. J. Polysulfone ultrafiltration membranes impregnated with silver nanoparticles show improved biofouling resistance and virus removal. *Water research* **2009**, *43*, 715-723.
(44) Sinclair, T.; Robles, D.; Raza, B.; van den Hengel, S.; Rutjes, S.; de Roda Husman, A.; de Grooth, J.; de Vos, W.; Roesink, H. Virus reduction through microfiltration membranes modified with a cationic polymer for drinking water applications. *Colloids and surfaces A: Physicochemical and engineering aspects* **2018**, *551*, 33-41.
(45) Szekeres, G. P.; Németh, Z. n.; Schrantz, K.; Németh, K. n.; Schabikowski, M.; Traber, J.; Pronk, W.; Hernádi, K. r.; Graule, T. Copper-coated cellulose-based water filters for virus retention. *ACS omega* **2018**, *3*, 446-454.
(46) Mostafavi, S.; Mehrnia, M.; Rashidi, A. Preparation of nanofilter from carbon nanotubes for application in virus removal from water. *Desalination* **2009**, *238*, 271-280.
(47) Rahaman, M. S.; Vecitis, C. D.; Elimelech, M. Electrochemical carbon-nanotube filter performance toward virus removal and inactivation in the presence of natural organic matter. *Environmental science & technology* **2012**, *46*, 1556-1564.
(48) Metreveli, G.; Wågberg, L.; Emmoth, E.; Belák, S.; Strømme, M.; Mihranyan, A. A Size-Exclusion Nanocellulose Filter Paper for Virus Removal. *Advanced healthcare materials* **2014**, *3*, 1546-1550.
(49) Sato, A.; Wang, R.; Ma, H.; Hsiao, B. S.; Chu, B. Novel nanofibrous scaffolds for water filtration with bacteria and virus removal capability. *Journal of electron microscopy* **2011**, *60*, 201-209.
(50) Ma, H.; Burger, C.; Hsiao, B. S.; Chu, B. Ultrafine polysaccharide nanofibrous membranes for water purification. *Biomacromolecules* **2011**, *12*, 970-976.

(51) Mauter, M. S.; Zucker, I.; Perreault, F.; Werber, J. R.; Kim, J.-H.; Elimelech, M. The role of nanotechnology in tackling global water challenges. *Nature Sustainability* **2018**, *1*, 166.

(52) Fuglie, L. J. The miracle tree: Moringa oleifera, natural nutrition for the tropics. **1999**.

(53) Ndabigengesere, A.; Narasiah, K. S.; Talbot, B. G. Active agents and mechanism of coagulation of turbid waters using Moringa oleifera. *Water research* **1995**, *29*, 703-710.

(54) Neto, J. X.; Pereira, M. L.; Oliveira, J. T.; Rocha-Bezerra, L. C.; Lopes, T. D.; Costa, H. P.; Sousa, D. O.; Rocha, B. A.; Grangeiro, T. B.; Freire, J. E. A Chitin-binding Protein Purified from Moringa oleifera Seeds Presents Anticandidal Activity by Increasing Cell Membrane Permeability and Reactive Oxygen Species Production. *Frontiers in Microbiology* **2017**, *8*, 980.

(55) Gassenschmidt, U.; Jany, K. D.; Bernhard, T.; Niebergall, H. Isolation and characterization of a flocculating protein from Moringa oleifera Lam. *Biochimica et Biophysica Acta (BBA)-General Subjects* **1995**, *1243*, 477-481.

(56) Gifoni, J. M.; Oliveira, J. T.; Oliveira, H. D.; Batista, A. B.; Pereira, M. L.; Gomes, A. S.; Oliveira, H. P.; Grangeiro, T. B.; Vasconcelos, I. M. A novel chitin-binding protein from Moringa oleifera seed with potential for plant disease control. *Peptide Science* **2012**, *98*, 406-415.

(57) Shebek, K.; Schantz, A. B.; Sines, I.; Lauser, K.; Velegol, S.; Kumar, M. The flocculating cationic polypetide from Moringa oleifera seeds damages bacterial cell membranes by causing membrane fusion. *Langmuir* **2015**, *31*, 4496-4502.

(58) Batista, A. B.; Oliveira, J. T.; Gifoni, J. M.; Pereira, M. L.; Almeida, M. G.; Gomes, V. M.; Da Cunha, M.; Ribeiro, S. F.; Dias, G. B.; Beltramini, L. M. New insights into the structure and mode of action of Mo-CBP3, an antifungal chitin-binding protein of Moringa oleifera seeds. *PloS one* **2014**, *9*, e111427.

(59) Freire, J. E.; Vasconcelos, I. M.; Moreno, F. B.; Batista, A. B.; Lobo, M. D.; Pereira, M. L.; Lima, J. P.; Almeida, R. V.; Sousa, A. J.; Monteiro-Moreira, A. C. Mo-CBP3, an antifungal chitin-binding protein from Moringa oleifera seeds, is a member of the 2S albumin family. *PLoS One* **2015**, *10*, e0119871.

(60) Sánchez-Martín, J.; Ghebremichael, K.; Beltrán-Heredia, J. Comparison of single-step and two-step purified coagulants from Moringa oleifera seed for turbidity and DOC removal. *Bioresource technology* **2010**, *101*, 6259-6261.

(61) Jerri, H. A.; Adolfsen, K. J.; McCullough, L. R.; Velegol, D.; Velegol, S. B. Antimicrobial sand via adsorption of cationic Moringa oleifera protein. *Langmuir* **2011**, *28*, 2262-2268.

(62) Xiong, B.; Piechowicz, B.; Wang, Z.; Marinaro, R.; Clement, E.; Carlin, T.; Uliana, A.; Kumar, M.; Velegol, S. B. Moringa oleifera f-sand filters for sustainable water purification. *Environmental Science & Technology Letters* **2017**, *5*, 38-42.

(63) Amarasiri, M.; Kitajima, M.; Nguyen, T. H.; Okabe, S.; Sano, D. Bacteriophage removal efficiency as a validation and operational monitoring tool for virus reduction in wastewater reclamation. *Water research* **2017**, *121*, 258-269.

(64) Pouillot, R.; Van Doren, J. M.; Woods, J.; Plante, D.; Smith, M.; Goblick, G.; Roberts, C.; Locas, A.; Hajen, W.; Stobo, J. Meta-analysis of the reduction of norovirus and male-specific coliphage concentrations in wastewater treatment plants. *Appl. Environ. Microbiol.* **2015**, *81*, 4669-4681.

(65) Adams, M. H. Bacteriophages. *Bacteriophages.* **1959**.
(66) Weber, K.; Osborn, M. The reliability of molecular weight determinations by dodecyl sulfate-polyacrylamide gel electrophoresis. *Journal of Biological Chemistry* **1969**, *244*, 4406-4412.
(67) ElHadidy, A. M.; Peldszus, S.; Van Dyke, M. I. An evaluation of virus removal mechanisms by ultrafiltration membranes using MS2 and ϕX174 bacteriophage. *Separation and Purification Technology* **2013**, *120*, 215-223.
(68) Jacangelo, J. G.; Adham, S. S.; Laîné, J. M. Mechanism of Cryptosporidium, Giardia, and MS2 virus removal by MF and UF. *Journal-American Water Works Association* **1995**, *87*, 107-121.
(69) Ullah, A.; Mariutti, R. B.; Masood, R.; Caruso, I. P.; Costa, G. H. G.; de Freita, C. M.; Santos, C. R.; Zanphorlin, L. M.; Mutton, M. J. R.; Murakami, M. T. Crystal structure of mature 2S albumin from Moringa oleifera seeds. *Biochemical and biophysical research communications* **2015**, *468*, 365-371.
(70) Chowdhury, R.; Ren, T.; Shankla, M.; Decker, K.; Grisewood, M.; Prabhakar, J.; Baker, C.; Golbeck, J. H.; Aksimentiev, A.; Kumar, M. PoreDesigner for tuning solute selectivity in a robust and highly permeable outer membrane pore. *Nature communications* **2018**, *9*, 3661.
(71) Chowdhury, R.; Allan, M.; Maranas, C. OptMAVEn-2.0: de novo design of variable antibody regions against targeted antigen epitopes. *Antibodies* **2018**, *7*, 23.
(72) Nordmark, B. A.; Bechtel, T. M.; Riley, J. K.; Velegol, D.; Velegol, S. B.; Przybycien, T. M.; Tilton, R. D. Moringa oleifera Seed Protein Adsorption to Silica: Effects of Water Hardness, Fractionation, and Fatty Acid Extraction. *Langmuir* **2018**, *34*, 4852-4860.
(73) Vélez-Gavilán, J. CABI. Moringa oleifera [Jeanine Vélez-Gavilán]. In: Invasive Species Compendium. Wallingford, UK: CAB International. www.cabi.org/isc. 2017.
(74) Hualin, P. C. https://commons.wikimedia.org/wiki/File:The_tree_and_seedpods_of_Moringa_oleifera.JPG. Accessed on 10/07/2019.